condensed matter

MDPI

Article

First-Principles Calculation of Copper Oxide Superconductors That Supports the Kamimura-Suwa Model

Hiroshi Kamimura [1,*], Masaaki Araidai [2], Kunio Ishida [3], Shunichi Matsuno [4], Hideaki Sakata [5], Kenji Shiraishi [2], Osamu Sugino [6] and Jaw-Shen Tsai [5,7]

1 Tokyo University of Science,1-3 Kagurazaka, Shinjuku-ku, Tokyo 162-8601, Japan
2 Institute of Materials and Systems for Sustainability, Nagoya University, Furo-cho, Chikusa-ku, Nagoya 464-8601, Japan; araidai@nagoya-u.jp (M.A.); shiraishi@cse.nagoya-u.ac.jp (K.S.)
3 Graduate School of Engineering, Utsunomiya University, Yoto, Utsunomiya, Tochigi 321-8585, Japan; ishd_kn@cc.utsunomiya-u.ac.jp
4 School Marine Science and Technology, Tokai University, Shimizu 424-8610, Japan; smatsuno@scc.u-tokai.ac.jp
5 Department of Physics, Faculty of Science, Tokyo University of Science,1-3 Kagurazaka, Shinjuku-ku, Tokyo 162-8601, Japan; sakata@rs.kagu.tus.ac.jp (H.S.); tsai@riken.jp (J.-S.T.)
6 Institute for Solid State Physics, The University of Tokyo, 5-1-5 Kashiwanoha, Kashiwa, Chiba 277-8581, Japan; sugino@issp.u-tokyo.ac.jp
7 RIKEN Center for Emergent Matter Science (CEMS), Wako, Saitama 351-0198, Japan
* Correspondence: kamimura@rs.kagu.tus.ac.jp

Received: 27 September 2020; Accepted: 22 October 2020; Published: 2 November 2020

Abstract: In 1986 Bednorz and Műller discovered high temperature superconductivity in copper oxides by chemically doping holes into La_2CuO_4 (LCO), the antiferromagnetic insulator. Despite intense experimental and theoretical research during the past 34 years, no general consensus on the electronic-spin structures and the origin of pseudogap has been obtained. In this circumstance, we performed a first-principles calculation of underdoped cuprate superconductors $La_{2-x}Sr_xCuO_4$ (LSCO) within the meta-generalized gradient approximation of the density functional theory. Our calculations clarify first the important role of the anti Jahn-Teller (JT) effect, the backward deformation against the JT distortion in La_2CuO_4 by doping extra holes. The resulting electronic structure agrees with the two-component theory provided by the tight-binding model of Kamimura and Suwa (K–S), which has been also used to elucidate the *d*-wave superconductivity. Our first-principles calculation thus justifies the K–S model and demonstrates advanced understanding of cuprates. For example, the remarkable feature of our calculations is the appearance of the spin-polarized band with a nearly flat-band character, showing the peaky nature in the density of states at the Fermi level.

Keywords: cuprates; LSCO; anti-Jahn-Teller effect; first-principles calculation; Kamimura-Suwa model; spin-polarized band; Hund's coupling spin-triplet and spin-singlet multiplets

1. Prologue by Hiroshi Kamimura

In 1987, Georg Bednorz and Alex Műller received the Nobel Prize in Physics for "their discovery of new superconducting materials". In 1988, the Steering Committee of NEC Symposium on Fundamental Approaches to the New Material Phases decided to choose "Mechanism of High Temperature Superconductivity" as the subject of the second NEC Symposium. This Symposium was held in Hakone, near Mt. Fuji, Japan on 24–27 October 1988. Alex was chosen as a plenary speaker, and I was the Symposium chairperson. The Symposium's group photo is shown in Figure 1.

Figure 1. Symposium's group photo in the front of the Hakone Kanko Hotel.

In 2005, we organized the International Workshop on Electronic Structure and Lattice Effects in Cuprates on October 27 and 28 in the National Institute of Advanced Industrial Science and Technology (AIST) in Tsukuba. Alex was a plenary speaker, and a number of Alex's friends, companions, colleagues, and former students attended this Workshop (see Figure 2).

Figure 2. International Workshop's group photo in the front of the Conference Hall in AIST.

On 27–28 March 2006, the International Symposium in Honor of J.G. Bednorz and K.A. Műller was held in University of Zurich, celebrating their discovery of cuprate superconductors 20 years ago. From Japan, six HTSC researchers, Yoichi Ando, Masatoshi Arai, Yoshiteru Maeno, Hiroyuki Oyanagi, Masaki Takashige, and Hiroshi Kamimura were invited. The group photo is shown below in Figure 3.

Figure 3. International Symposium' group photo. The front row: From the left, Prof. Hugo Keller, Prof. Alex Műller, Dr. Georg Bednorz, Prof. Hiroshi Kamimura.

2. Introduction

By the discovery of high-temperature superconductivity (HTSC) in cuprates by Bednorz and Műller [1,2], it is well known that cuprate superconductors are different from ordinary metallic superconductors in the production process of carriers. Cuprates are ionic crystals. The carriers in La_2CuO_4, an antiferromagnetic insulator [3], are produced from doping chemical elements or making oxygen deficiencies, for example, by replacing 3+ cations (La^{3+}) by 2+ ones (Sr^{2+}) in $La_{2-x}Sr_x$ CuO_4 (LSCO). Thus, the electronic structures of cuprate superconductors may vary drastically upon doping holes [4].

In this circumstance, we pay attention to the experimental facts that a CuO_6 octahedron in a parent material La_2CuO_4 is deformed into an elongated shape (tetragonal) due to the Jahn–Teller (JT) theorem for an orbitally doubly degenerate state of a Cu^{2+} ion [1,5]. When extra holes are doped, the apical O^{2-} ions in elongated CuO_6 octahedrons in LCO tend to approach toward Cu^{2+} ions to gain the attractive electrostatic energy [6]. This backward deformation against the JT deformations is called the anti-JT effect [7,8]. As a result, the energy separation between the two JT-split levels becomes smaller, i.e., pseudo-degenerate. This anti-JT effect in cuprates was supported experimentally by the neutron scattering [9] and the polarization-dependent spectroscopy [10,11].

Under these circumstances, there are two views concerning the electronic structures of LSCO. One view is based on the single-component theory in which only orbitals extended in a CuO_2 plane are considered. Since a doped hole moves within a CuO_2 plane, this model is irrelevant to the anti-JT effect. A typical model to take this view is the *t*-J model [12,13].

An alternative view is based on the two-component theory initiated by the Kamimura–Suwa (K–S) model [14,15], in which the two kinds of molecular orbitals (MOs) of each CuO_6 octahedron parallel and perpendicular to a CuO_2 plane are considered. Those MOs are $|a^*_{1g}>$ antibonding and $|b_{1g}>$ bonding orbitals, as shown in Figure 4. In this figure, the schematic MO levels, b_{1g} bonding, a^*_{1g} antibonding, and b^*_{1g} antibonding orbitals, and the hole configurations in Hund's coupling multiplet $^3B_{1g}$ and spin-singlet multiplet $^1A_{1g}$ are shown. On the left side of the figure, a hole occupying a^*_{1g} orbital (red arrow) aligns its spin in parallel to the up spin of a localized hole occupying the b^*_{1g} orbital (green arrow) to form $^3B_{1g}$, owing to the Hund's coupling exchange interaction with the coupling constant, K_{a1g} (−2 eV) [16].

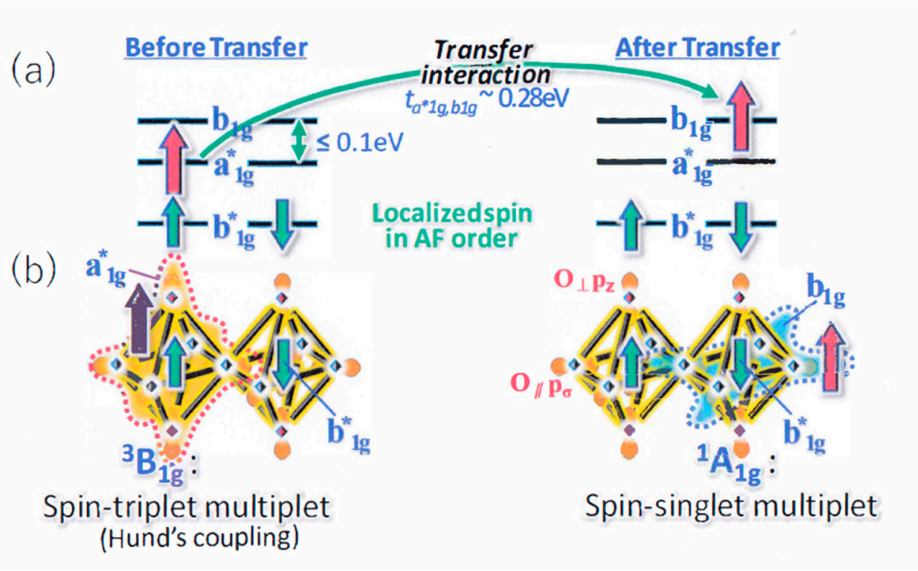

Figure 4. The K–S model: the coexistence of a metallic state and the AF order. In this figure, (**a**) the transfer (*a long curved arrow*) of a doped hole (red arrows) from $^3B_{1g}$ to $^1A_{1g}$ without destroying the AF order is shown, and (**b**) the spatial extension of a^*_{1g} MO (left side) and b_{1g} MO (right side) are shown, where $O_{/\!/}$ and $O_\perp$ represent in-plane and apical oxygen, respectively.

On the other hand, on the right side of the figure, a hole occupying the b_{1g} level (up red arrow) forms a spin-singlet (SS) multiplet with the down spin of a localized hole occupying the b^*_{1g} level (green arrow), $^1A_{1g}$, owing to the larger exchange coupling K_{b1g} (= 4 eV) [16]. The key-feature of the K–S model is the coexistence of a metallic state and the AF order.

The above two types of exchange interaction, the Hund's coupling spin-triplet and the spin-singlet (SS), can be described by the scalar product of the spin of the localized $|b^*_{1g}>$ hole, S_i, and that of the itinerant $|a^*_{1g}>$ or $|b_{1g}>$ hole, $s_{i,a^*_{1g}}$ or $s_{i,b_{1g}}$, at each CuO_6 site, i, yielding the Hamiltonian interaction

$$H_{ex} = \sum_i \left(K_{a^*_{1g}} s_{i,a^*_{1g}} \cdot S_i + K_{b_{1g}} s_{i,b_{1g}} \cdot S_i \right). \quad (1)$$

This Hamiltonian interaction constitutes the K–S Hamiltonian to describe the K–S model, in which the localized spins form an AF order [14,15]. The whole K–S Hamiltonian is shown below.

$$\begin{aligned} H &= H_{orbital} + H_{tr} + H_{AF} + H_{ex} \\ &= \sum_{im\sigma} \varepsilon_m c^+_{im\sigma} c_{im\sigma} + \sum_{(i,j)mn\sigma} t_{mn} (c^+_{im\sigma} c_{jn\sigma} + h.c.) + J \sum_{(i,j)} S_i \bullet S_j + \sum_{im} K_m s_{im} \bullet S_i \,, \end{aligned} \quad (2)$$

where ε_m (m = a_{1g}*, or b_{1g}) represents the one-electron energy of the a^*_{1g} or b_{1g} MO states, $C^\dagger_{im\sigma}$ and $C_{im\sigma}$ are the creation and annihilation operators of a doped hole in the m-type MO with spin σ in the i-th CuO_6 octahedron, respectively, t_{mn} is the transfer integral of a doped hole between the m- and n- type MOs of neighboring CuO_6 octahedrons, J the superexchange interacrion (as regards the details of the K–S Hamiltonian, see Ref. [17]).

3. First-Principles Calculations

In order to decide whether the one-component t–J model or the two-component K–S model is suitable to describe the electronic-spin state of cuprates, Kamimura et al. [18] recently performed the first-principles non-empirical calculation. In their calculations, the first-principle method of the constrained-and-appropriately normed (SCAN) density functional was adopted to calculate a non-rigid electronic-spin energy bands of LCO and LSCO, following Furness et al. [19]. Kohn-Sham density

functional theory (DFT) is a widely-used electronic structure theory for materials as well as condensed matters. This SCAN method is more useful for the electronic-spin structures of diversely-bonded materials (including covalent, metallic, ionic, Jahn-Teller deformed bonds, cuprates consisting of CuO_6 octahedrons and CuO_5 pyramids).

The purpose of this contribution is to show how the first-principles SCAN calculations agree with the K–S model in the tight binding form. In the first-principles calculations, a unique method was adopted—that is, to investigate the electronic states of LSCO by calculating both the energy bands in *k*-space and the wavefunctions in *r*-space simultaneously. For this purpose, we calculated not only the non-rigid energy band and the density of states (DOS) in *k*-space but also the partial DOS (PDOS) which gives information on MOs in a CuO_6 octahedron in *r*-space. Here PDOS means the density of states projected to the wavefunctions, or orbitals.

4. Calculated Results

4.1. La_2CuO_4 (LCO): Antiferromagnetic (AF) Insulator

The La_2CuO_4 (LCO) transforms from the high temperature tetragonal phase (HTT) into the low temperature orthorhombic phase (LTO) when temperature decreases. The calculated results on the crystal structure explains the Jahn–Teller distortion of an elongated octahedron. The calculated Cu magnetic moment, 0.510 μ_B, is in agreement with the observed values of 0.50 μ_B [20,21]. This means that the DFT-SCAN method [18,19] treats the spin-fluctuation effect properly. The calculated result shows that LCO is the antiferromagnetic insulator.

4.2. $La_{2-x}Sr_x$ CuO_4 (LSCO)

In order to calculate the non-rigid energy bands for LSCO with AF order [22], the $2\sqrt{2} \times 2\sqrt{2}$ supercell is adopted, in which there are two CuO_2 planes and each CuO_2 plane includes eight CuO_6 octahedrons. The Brillouin zone (BZ) for this $2\sqrt{2} \times 2\sqrt{2}$ supercell is shown in Figure 5. In this supercell, we cannot discuss the stability of stripe phases which were recently reported by Zhang et al. for YBCO systems [23].

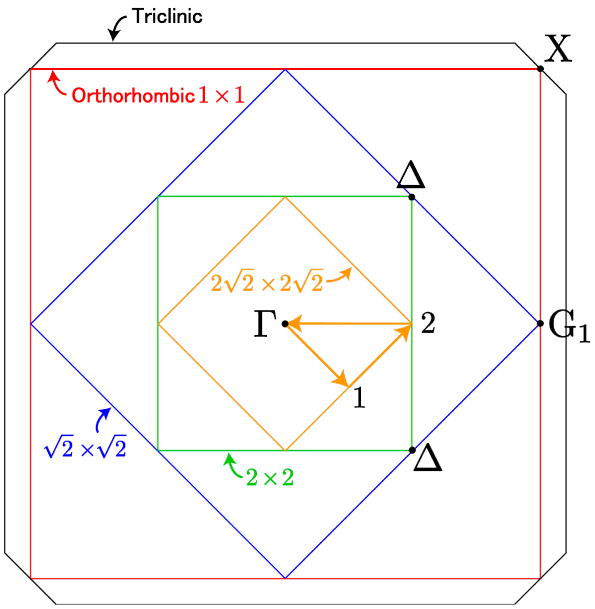

Figure 5. The Brillouin zone (BZ) for the $2\sqrt{2} \times 2\sqrt{2}$ supercell. Inside the BZ, a special triangle root starting form Γ is shown, where the special points 1 and 2 are used later in Figure 10.

Here we show that the key points obtained from the first-principles calculations for LSCO agree with those of the K–S model shown in Figure 4. In particular, it is shown that the Hund's coupling spin-triplet in the K–S model agrees with the appearance of a spin-polarized band in cuprates.

4.3. A Metallic Phase with x = 0.125 (the Underdoped Regime)

In this case, Sr is substituted for one La in each CuO_2 plane in the supercell, leading to $x = 0.125$. The calculated Cu and apical O shortest distance in a CuO_6 octahedron in LSCO is 2.216 Å, which is considerably smaller than 2.448 Å in LCO. This shrinkage of the Cu and apical O distance by doping holes indicates that the anti-JT effect really occurs in LSCO. This result also supports the K–S model.

Although the calculated magnetization at each Cu site suggests the existence of AF order, the calculated value at each site takes a different value. For example, among the calculated values of the magnetization at each Cu site in Figure 6, the absolute value at Cu_4 site shows the maximum value of 0.643 μ_B, which is considerably larger than the magnetization at a Cu site in LCO, 0.510 μ_B. Here we discuss the origin of the high value of magnetization, 0.643 μ_B in LSCO with $x = 0.125$.

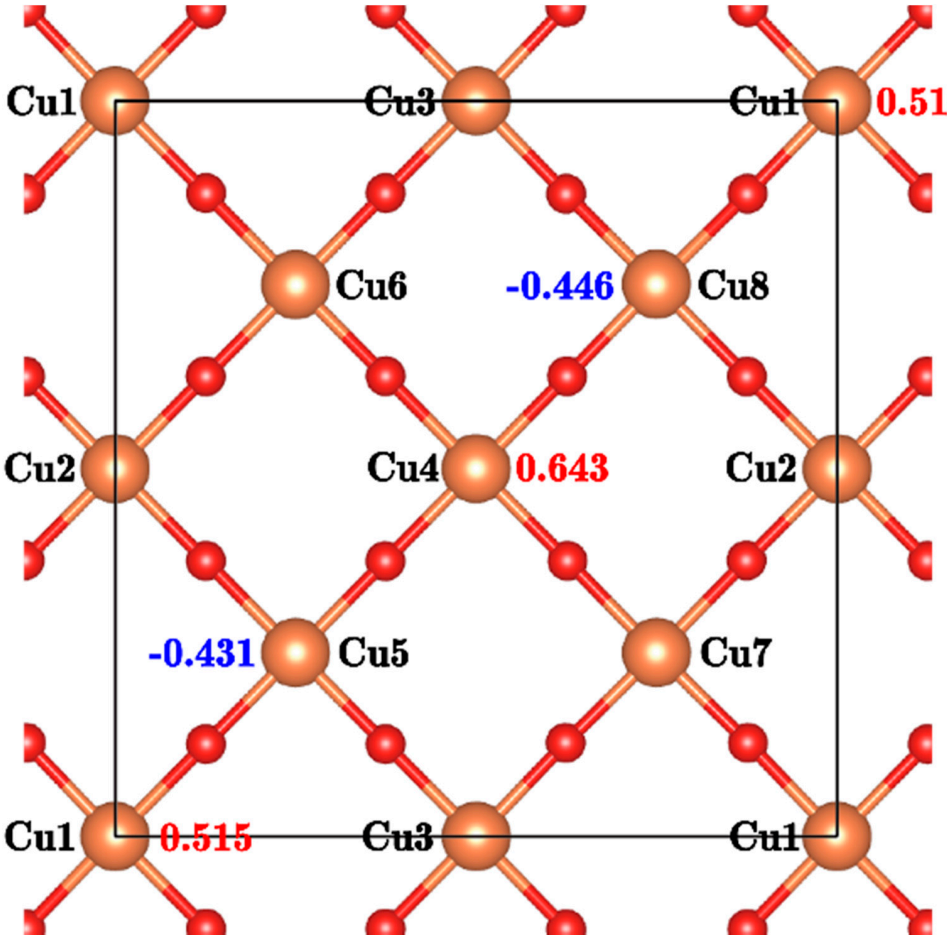

Figure 6. The calculated magnetization at each Cu site in $La_{2-x}Sr_x$ CuO_4 (LSCO) with $x = 0.125$.

In order to obtain information on the wavefunctions in a CuO_6 octahedron, the PDOS (partial density of states) of dz^2 orbital and its ligand O p_z orbitals in a CuO_6 octahedron at the Cu_4 site is calculated. The calculated results are shown in Figure 7. Using these orbitals in a CuO_6 octahedron at the Cu_4 site, an antibonding $|a^*_{1g}>$ MO is constructed, in order to investigate a relation between the $|a^*_{1g}>$ orbital in the energy band and the antibonding $|a^*_{1g}>$ MO in the K–S model in Figure 4, where Cu in CuO_6 octahedron is assigned to Cu_4.

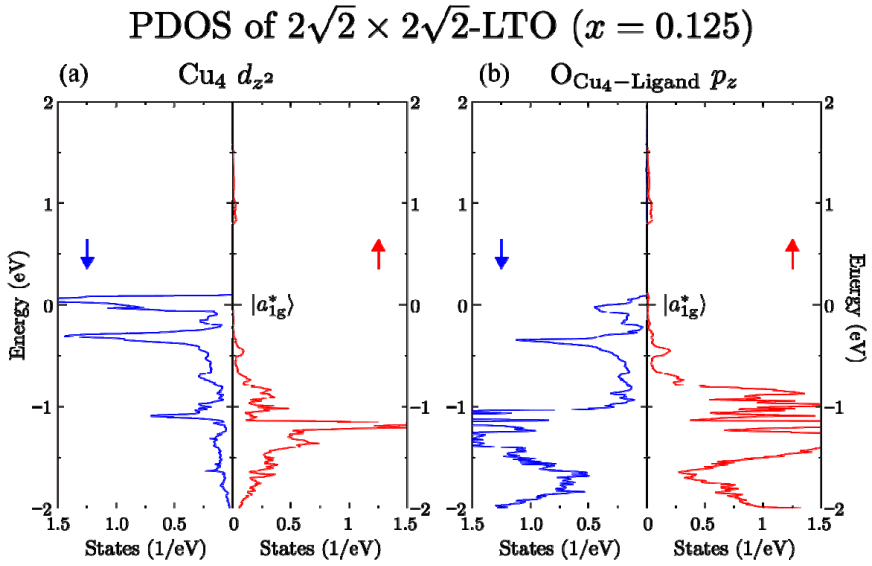

Figure 7. Calculated partial density of states (PDOS) of orbitals in CuO_6 at Cu_4 site: energy 0 is E_F. (**a**) PDOS of Cu-dz^2 orbital; (**b**) PDOS of ligand apical O-p_z orbital.

4.4. The Close Relation between a Spin-Polarized Band in the First Principles Calculations and Hund's Coupling Spin Triplet in the K–S Model

4.4.1. The Appearance of a Spin-Polarized Band in Cuprates

Another remarkable feature of the highest hole band is the spin polarization at the Cu_4 site (Figure 7). The difference in the highest states between up-spin and down-spin bands is considered as the "ferromagnetic band splitting" discussed by Slater [24], and Connolly [25]. Indeed, according to the criterion for the occurrence of a spin-polarized band in LSCO derived in the paper [18], the Hund's coupling exchange interaction $K_{a^*_{1g}}(x)\vec{s}_{i,a^*_{1g}} \cdot \vec{S}_i$ in Equation (1) may cause a spin-polarized band when $K(x)D(E_F) > 1$, where $K(x) = |K_{a^*1g}(x)|$ and $D(E_F)$ is the density of states at E_F. The magnitude of $K(x)$ is 2.0 eV for LCO ($x = 0$) and is larger in LSCO because of the anti-JT effect. Figure 7 shows that $D(E_F)$ is much larger than 1.5 states/eV. Thus, the condition for the appearance of the spin-polarized band is satisfied. We also notice that the PDOS of the highest down-spin Cu_4 dz^2 hole band in Figure 7a, i.e., the spin-polarized band, shows a "peaky" nature due to the existence of a nearly-flat highest hole band, which originates from the JT and the anti-JT deformations. In fact, the effective mass of a hole carrier in this band is six times heavier than the free electron mass. Thus, we consider that this hole carrier is a "*Jahn-Teller polaron*", proposed by Alex [26–28]. We expect that the peaky nature may be observed for underdoped LSCO by performing an STM or STS measurement

4.4.2. Relation between the Cu_4 dz^2 Band and the Hund's Coupling Spin-Triplet in the K–S Model

Now, in order to investigate whether a doped hole in the Cu_4 dz^2 band($|a^*_{1g}>$ MO) forms the Hund's coupling spin-triplet $^3B_{1g}$ with a localized spin at the same Cu_4 site, we calculated the PDOS of Cu_4 dx^2-y^2 and ligand O-p_x, p_y orbitals in x-y plane, which form the antibonding $|b^*_{1g}>$ MO and the bonding $|b_{1g}>$ MO in a CuO_6 octahedron. The calculated results are shown in Figure 8. The Cu_4 dx^2-y^2 orbital and the ligand O-p_x, p_y orbitals that appear in the energy region of 1 to 2eV above E_F in Figure 8 form the antibonding $|b^*_{1g}>$ MO. This MO is occupied by the localized holes with down spins. Since both spins of the localized holes in $|b^*_{1g}>$ MO and of the doped holes in the Cu_4 dz^2 band ($|a^*_{1g}>$ MO) take the same direction, down spins, the total magnetization at the Cu_4 site becomes the maximum value of $0.643\mu_B$. Thus, one can conclude that the Hund's coupling between a localized hole in $|b^*_{1g}>$ MO and a doped hole in the Cu_4 dz^2 band ($|a^*_{1g}>$ MO) plays an important role in LSCO with x = 0.125 in the first-principles calculations.

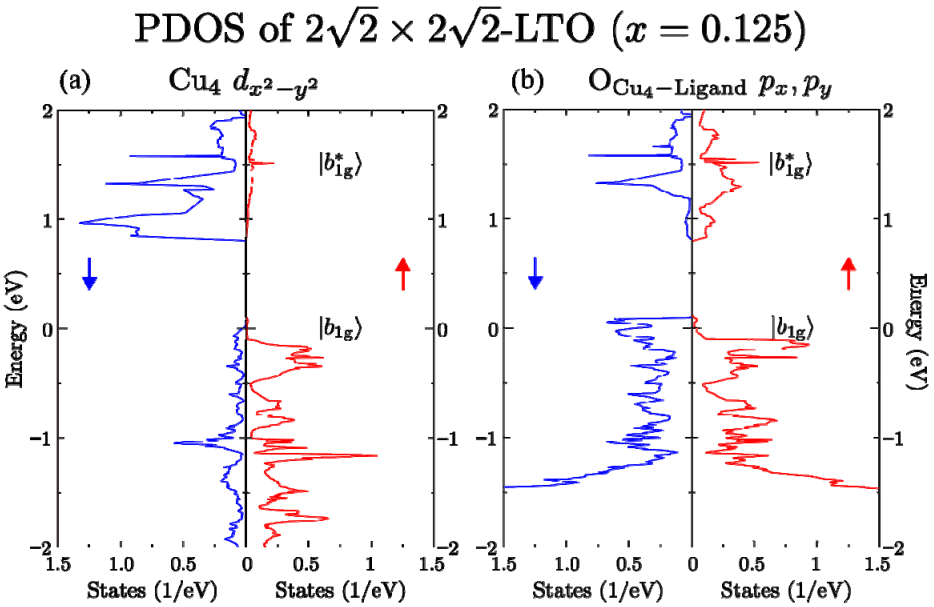

Figure 8. Calculated PDOS of orbitals in CuO_6 at Cu_4 site: Energy 0 is E_F. (**a**) PDOS of Cu-dx^2-dy^2 orbital; (**b**) PDOS of ligand in-plane-O p_x, p_y orbitals.

4.4.3. Itinerancy of a Hole in the Cu_4 dz^2 Band

The present first-principle calculations also show how a doped hole in the Cu_4 dz^2 band ($|a^*_{1g}>$ MO) itinerates in LSCO in the underdoped regime.

Let us pay attention to the hopping of a doped hole with down spin from a Cu_4 site to a neighboring Cu_8 site in the AF order, whose magnetization, $-0.446\mu_B$, is opposite to that at the Cu_4 site, $+0.643$ μ_B. We calculated the PDOS of Cu-dx^2-y^2 orbital and ligand O-p_x, p_y orbitals in the x–y plane at the neighboring Cu_8 site, as shown in Figure 9. In this figure, we find that these orbitals form bonding b_{1g} and antibonding b^*_{1g} MOs in a CuO_6 octahedron at the Cu_8 site. The $|b^*_{1g}>$ MO with Cu-dx^2-y^2 (a localized hole) appears in the energy region of 1 to 2 eV above E_F (red color) in Figure 9a while the $|b_{1g}>$ MO (a doped hole) appears just above E_F. By comparing the calculated results of the spin-direction of a localized hole in Figure 9a (red color) with that in Figure 8a (blue color), we notice that the localized spins at the Cu_8 site are directed upwards, while those at the Cu_4 site are opposite in the spin directions. Thus, we conclude that the AF order is not destroyed during the itinerancy of a doped hole in LSCO.

Furthermore, when a hole with down spin in the Cu_4 dz^2 band ($|a^*_{1g}>$ MO) at the Cu_4 site hops into a neighboring Cu_8 site in the AF order, the first-principles calculation shows that this hole enters an empty $|b_{1g}>$ MO just above E_F at the Cu_8 site, taking a spin antiparallel configuration (the spin-singlet) with the localized hole in $|b^*_{1g}>$ MO at the same site (see Figure 9).

4.4.4. Good Agreement between the First-Principles SCAN Calculations and the K–S Model in the Tight-Binding Form

Summarizing the itinerancy of a doped hole from Cu_4 dz^2 orbital to Cu_8 dx^2-y^2 orbital, the spin-state of the doped hole changes from the Hund' coupling spin-triplet with the localized spin at Cu_4 site to the spin-singlet with the localized spin at Cu_8 site.

This itinerancy of a doped hole in the first-principles SCAN calculations is strikingly consistent with the K–S model. In the K–S model (see Figure 4), when a doped hole with up spin enters a Cu site with a up localized spin in b^*_{1g} MO, it occupies an a^*_{1g} MO to align its spin in parallel with the up spin of a localized hole in the b^*_{1g} MO to form $^3B_{1g}$, owing to the Hund's coupling exchange interaction, and owing to the transfer interactions, hops to the b_{1g} MO of a neighboring Cu site in the AF order taking antiparallel spin configuration with the localized spin. By repeating this transfer

process, a doped hole itinerates in LSCO without destroying the AF order. We call this doped hole a "KS particle".

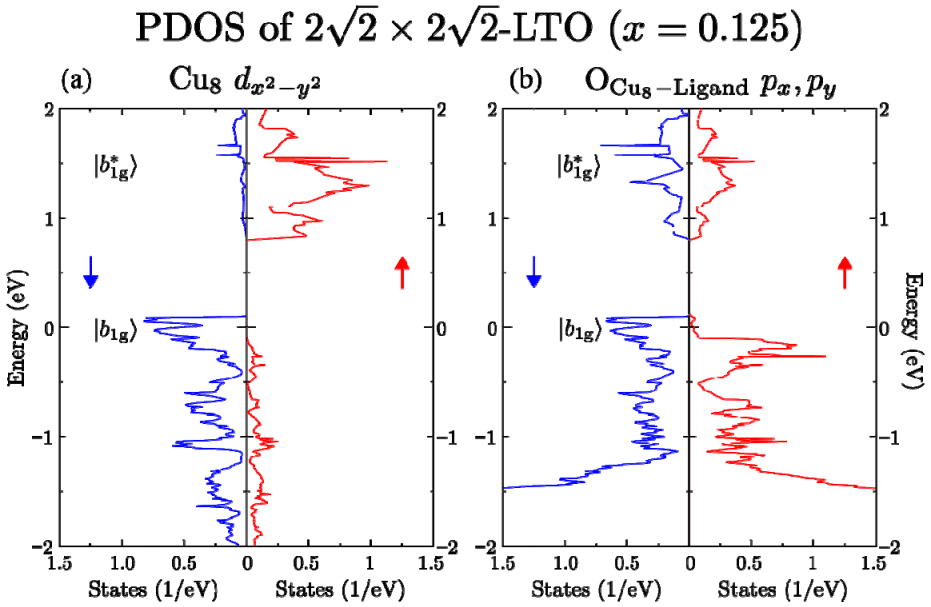

Figure 9. Calculated PDOS of orbitals in CuO_6 at Cu_8 site: (**a**) PDOS of Cu-dx^2-dy^2 orbital; (**b**) PDOS of ligand in-plane-O p_x, p_y orbitals. Energy 0 is E_F.

Thus, we understand that the first-principle SCAN calculation is in good agreement with the K–S model in the tight-binding form [14,15]. Namely, in LSCO a doped hole itinerates by taking the Hund's coupling and the spin-singlet states alternately without destroying the AF order.

4.5. Construction of Fermi Surfaces of LSCO with x = 0.125

Based on the present first-principle SCAN calculated results for $x = 0.125$, we construct a Fermi surface (FS) in the underdoped LSCO. In doing so, we would like to point out one problem in our supercell model. In the supercell, a size of a unit cell is wider than that of an ordinal LSCO crystal with the LTO phase. As seen in BZs for various supercell-models in Figure 5, the BZ of a supercell is obtained by folding that of a regular crystal, as shown in Figure 5. As a result, in the case of $2\sqrt{2} \times 2\sqrt{2}$ model, the symmetry points $\Gamma(0, 0)$, $X(\pi,\pi)$, $G_1(\pi, 0)$, and $\Delta(\pi/2, \pi/2)$ gather at Γ. Thus, one may have a difficulty in assigning each calculated energy band to either of symmetry points Γ, X, G_1, and Δ.

As an example, we show the calculated energy bands and DOS of LSCO with $x = 0.125$ in Figure 10. In this figure one may notice that there are two hole-bands above E_F, and that the DOS of the second highest hole-band is very large and peaky shape. Since the peaky shape of DOS is originated from the spin-polarized band $|a^*_{1g}>$ in Figure 7 and the spin-polarized band appears at $G_1(\pi, 0)$ in k space, we assign this hole band to a symmetry point $G_1(\pi, 0)$. On the other hand, we also pay attention to a doped hole in the highest hole-band ($|b_{1g}>$) and a localized hole in the band ($|b^*_{1g}>$) in the energy 1 to 2 eV above E_F in Figure 8b. These holes form an SS (spin-singlet) particle (see Figure 4), and contribute to the formation of Fermi arcs at the Δ point in BZ.

Based on the above-mentioned results of the first-principles calculations, we construct the Fermi surface of LSCO with $x = 0.125$. The feature of the thus-obtained Fermi surface (FS) of LSCO with $x = 0.125$ in the underdoped regime is the coexistence of Fermi pockets (G_1 points) and Fermi arcs (Δ points), and the KS particles occupy the Fermi pockets while the SS particles occupy the Fermi arcs, as shown in Figure 11. This feature seems consistent with the experimental results of angle-resolved photoemission spectroscopy (ARPES) for LSCO with $x = 0.15$ by Yoshida et al. [29].

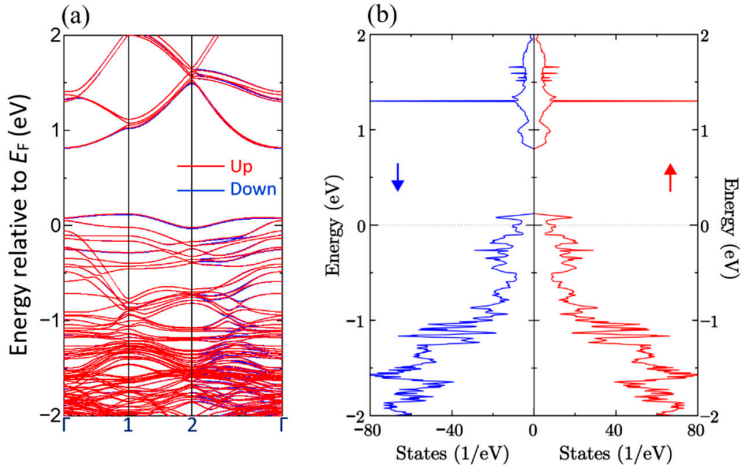

Figure 10. Spin-dependent Non-rigid energy bands and DOS of LSCO with $x = 0.125$. E_F is energy zero. (**a**) Energy bands. (**b**) DOS.

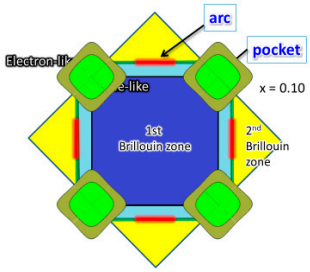

Figure 11. Fermi surface of LSCO with $x = 0.10$ (the underdoped regime).

5. Final Remarks

The feature of the obtained Fermi surface (FS) of LSCO with $x = 0.125$ in the underdoped regime mentioned in Section 4.5 is the coexistence of Fermi pockets (G_1 points) and Fermi arcs (Δ points), and the KS particles occupy the Fermi pockets while the SS particles occupy the Fermi arcs. We find that the FS for the underdoped LSCO (Figure 10) is similar to that of the K–S model [14,15], which is shown in Figure 11. This feature is likely to be consistent with the experimental results of angle-resolved photoemission spectroscopy (ARPES) for LSCO with $x = 0.15$ by Yoshida et al. [27]. Here, the wavefunctions of a KS particle with up and down spins, $\Psi_{k,\uparrow}(\boldsymbol{r})$ and $\Psi_{k,\downarrow}(\boldsymbol{r})$, have the unique phase relation [30],

$$\Psi_{k,\downarrow}(\boldsymbol{r}) = \exp(i\,\boldsymbol{k}\cdot\boldsymbol{a})\,\Psi_{k,\uparrow}(\boldsymbol{r}), \tag{3}$$

where $\boldsymbol{a}$ is a vector connecting Cu atoms along the Cu-O-Cu line.

Thus, the KS particles on the Fermi pockets around $G_1(\pi, 0)$ points contribute to the d-wave superconductivity in the phonon mechanism below Tc [30–33] (see also [4]).

6. Conclusions

In the present paper, we have shown that the K–S model is consistent with the first-principle method of the constrained-and-appropriately normed (SCAN) density functional. Furthermore, the Fermi-surfaces of LSCO in the underdoped region obtained from the first-principle SCAN density functional method coincide with those derived from the K–S model semi-empirically, so that one may consider that the theory of d-wave superconductivity developed by the K–S model [30] is justified by the first-principles theory.

Author Contributions: All authors contributed extensively to the work presented in this paper. M.A. carried out the DFT-SCAN computations. H.K., M.A. K.S., O.S., K.I. developed the non-rigid energy-band theory of correlated electrons in cuprates, especially the spin-dependent band theory, and compared with the K–S model in the tight binding form. S.M. developed the *d*-wave superconductivity based on the K–S model, H.S. and J.-S.T. compared theoretical results with experiments on STM, STS, interlayer tunneling experiments in cuprates. H.K. mainly wrote the manuscript. All authors discussed the results and commented on the manuscript. All authors have read and agreed to the published version of the manuscript.

Funding: This research received no external funding.

Acknowledgments: At this happy occasion of dedicating the present paper to Alex, I, Hiroshi kamimura, sincerely thank Alex for guiding me to our research on cuprates of the Jahn-Teller materials. We would like to thank Atsushi Fujimori, Kazuyoshi Yamada, Setsuo Mitsuda for their valuable discussion on experimental results. This work was supported by Tokyo University of Science. The computation was carried out in part using the computer resource offered under the category of General Projects by Research Institute for Information Technology, Kyushu University.

Conflicts of Interest: The authors declare no conflict of interest.

References

1. Bednorz, J.G.; Müller, K.A. Possible high Tc superconductivity in the Ba-La-Cu-O system. *Z. Phys. B* **1986**, *64*, 189–193.
2. Bednorz, J.G.; Müller, K.A. Perovskite-type oxides-the new approach to high- T_c superconductivity. *Rev. Mod. Phys.* **1988**, *60*, 585. [CrossRef]
3. Anderson, P.W. Resonating valence bond state in La_2CuO_4 and superconductivity. *Science* **1987**, *235*, 1196–1198. [CrossRef] [PubMed]
4. Kamimura, H.; Sugino, O.; Tsai, J.S.; Ushio, H. Jahn-Teller-effect induced superconductivity in copper oxides: Theoretical developments. In *High-T_c Copper Oxide Superconductors and Related Novel Materials, Dedicated to Prof. K.A. Müller on the Occasion of his 90th Birthday*; Bussmann-Holder, A., Keller, H., Bianconi, A., Eds.; Springer: Berlin/Heidelberg, Germany, 2017.
5. Sugano, S.; Tanabe, Y.; Kamimura, H. *Multiplets of Transition Metal U., and Ions in Crystals*; Chapter X; Academic Press: Cambridge, MA, USA, 1970.
6. Shima, N.; Shiraishi, K.; Nakayama, T.; Oshiyama, A.; Kamimura, H. Electronic structures of doped (La(1-x)Srx)2CuO4.in tetragonal phase. In Proceedings of the 1st International Conference on Electronic Materials Tokyo, June 1988: New Materials and New Physical Phenomena for Electronics of the 21st Century, Shigaku-Kaikan, Tokyo, Japan, 13–15 June 1988; Sugano, T., Chang, R.P.H., Kamimura, H., Hayashi, I., Kamiya, T., Eds.; Material Research Society: Pittsburgh, PA, USA, 1989; pp. 51–54.
7. Anisimov, V.L.; Ezhov, S.Y.; Rice, T.H. Singlet and triplet hole-doped configuration in $La_2Cu_{0.5}Li_{0.5}O_4$. *Phys. Rev. B* **1997**, *55*, 12829–12832. [CrossRef]
8. Kamimura, H.; Matsuno, S.; Mizokawa, T.; Sasaoka, K.; Shiraishi, K.; Ushio, H. On the important role of the anti-Jahn-Teller effect in underdoped cuprate superconductors. *J. Phys. Conf. Ser.* **2013**, *428*, 012043. [CrossRef]
9. Egami, T.; Toby, B.H.; Billinge, S.J.L.; Janot, C.; Jorgensen, J.D.; Hinks, D.G.; Subramanian, M.A.; Crawford, M.K.; Farneth, W.E.; McCarron, E.M. Local structural anomaly at T_c observed by neutron scattering. 389. In *High Temperature Superconductivity*; Ashkenazi, J., Barnes, J., Vezzoli, G.C., Klein, B.M., Eds.; Springer Science + Business Media, LLC.: New York, NY, USA, 1991.
10. Chen, C.T.; Tjeng, L.H.; Kwo, H.; Kao, L.; Rudolf, P.; Sette, P.; Fleming, R.M. Out-of-plane orbital characteristics of intrinsic and doped holes in $La_{2-x}Sr_xCuO_4$. *Phys. Rev. Lett.* **1992**, *68*, 2543–2546. [CrossRef] [PubMed]
11. Pellegrin, E.; Nücker, N.; Fink, J.; Molodtsov, S.L.; Gutierre, A.; Navas, E.; Sterebel, O.; Hu, Z.; Domke, M.; Kaindl, G.; et al. Greene, Orbital character of states at the Fermi level in $La_{2-x}Sr_xCuO_4$ and $R_{2-x}Ce_xCuO_4$ (R = Nd_2Sm). *Phys. Rev. B* **1993**, *47*, 3354–3367. [CrossRef]
12. Zhang, F.C.; Rice, T.M. Effective Hamiltonian for the superconducting Cu oxides. *Phys. Rev. B* **1988**, *37*, 3759–3761. [CrossRef]
13. Norman, M.R.; Kanigel, A.; Randeria, M.; Chtterjee, M.; Campuzano, J.C. Modeling the Fermi arc in underdoped cuprates. *Phys. Rev. B* **2007**, *76*, 174501. [CrossRef]
14. Kamimura, H.; Suwa, Y. New theoretical view for high temperature superconductivity. *J. Phys. Soc. Jpn.* **1993**, *62*, 3368–3371. [CrossRef]

15. Kamimura, H.; Hamada, T.; Ushio, H. Theoretical exploration of electronic structure in cuprates from electronic entropy. *Phys. Rev. B* **2002**, *66*, 054504. [CrossRef]
16. Kamimura, H.; Eto, M. $^1A_{1g}$ to $^3B_{1g}$ Conversion at the onset of superconductivity in $La_{2-x}Sr_xCuO_4$ due to the apical oxygen effect. *J. Phys. Soc. Jpn.* **1990**, *59*, 3053–3056. [CrossRef]
17. Kamimura, H.; Ushio, H.; Matusno, S.; Hamada, T. *Theory of Copper Oxide Superconductors*; Chapter 8.3; Springer: Berlin/Heidelberg, Germany, 2005.
18. Kamimura, H.; Sugino, O.; Shiraishi, K.; Araidai, M.; Tsai, J.S.; Sakata, H.; Ishida, K.; Matsuno, S. A First-Principles Non-Rigid Band Theory of Correlated Electrons in Copper Oxide Superconductors. 2020; In Preparation.
19. Furness, J.W.; Zhang, Y.; Lane, C.; Buda, I.G.; Barbielini, B.; Markiewicz, R.S.; Bansil, A.; Sun, J. An accurate first-principles treatment of doping-dependent electronic structure of high-temperature cuprate superconductors. *Commun. Phys.* **2018**, *1*, 11. [CrossRef]
20. Vaknin, D.; Sinha, S.K.; Moncton, D.E.; Johnson, D.C.; Newsam, J.; Safinya, C.R.; King, H. Antiferromagnetism in $La_2CuO_{4-\gamma}$. *Phys. Rev. Lett.* **1996**, *77*, 723–726.
21. Freltoft, T.; Shirane, G.; Mitsuda, S.; Remeika, J.P.; Cooper, A.S. Magnetic form factor of Cu in La_2CuO_4. *Phys. Rev. B* **1988**, *37*, 137. [CrossRef] [PubMed]
22. Yamada, K.; Lee, C.H.; Wada, J.; Kurahashi, K.; Kimura, H.; Endoh, Y.; Hosoya, S.; Shirane, G.; Birgeneau, R.J.; Kastner, M.A. Spatial modulation of low-frequency spin-fluctuation in hole-doped La_2CuO_4. *J. Supercond.* **1997**, *10*, 343. [CrossRef]
23. Zhang, Y.; Lane, C.; Furness, J.W.; Barbiellini, B.; Perdew, J.P.; Markiewicz, R.S.; Bansil, A.; Suna, J. Competing stripe and magnetic phases in the cuprates from first principles. *Proc. Nat. Acad. Sci. USA* **2020**, *117*, 68. [CrossRef]
24. Slater, J.C. The Ferromagnetism of Nickel. *Phys. Rev.* **1936**, *49*, 537. [CrossRef]
25. Connolly, J.W. Energy bands in ferromagnetic nickel. *Phys. Rev.* **1967**, *159*, 415. [CrossRef]
26. Műller, K.A. Large, small, and especially jahn-teller polarons. *J. Supercond.* **1999**, *12*, 3. [CrossRef]
27. Shengelaya, A.; Zhao, G.M.; Keller, H.; Műller, K.A. EPR evidence of Jahn-Teller polaron formation in $La_{1-x}Ca_xMnO_{3+y}$. *Phys. Rev. Lett.* **1996**, *77*, 5296. [CrossRef]
28. Lanzara, A.; Saini, N.L.; Brunelnelli, M.; Natali, F.; Bianconi, A.; Radaelli, P.G.; Cheong, S.W. Crossover from large to small polarons across the metal-insulator transition in manganites. *Phys. Rev. Lett.* **1998**, *81*, 878. [CrossRef]
29. Yoshida, T.; Zhou, X.J.; Tanaka, K.; Yang, W.L.; Hussain, Z.; Shen, Z.-X.; Fujimori, A.; Sahrakorpi, S.; Lindroos, M.; Markiewicz, R.S.; et al. Systematic doping evolution off underlying Fermi surface of $La_{2-x}Sr_xCuO_4$. *Phys. Rev. B* **2006**, *74*, 224510. [CrossRef]
30. Kamimura, H.; Matsuno, S.; Suwa, Y.; Ushio, H. Occurrence of *d*-wave pairing in the phonon-mediated mechanism of high temperature superconductivity in cuprates. *Phys. Rev. Lett.* **1996**, *77*, 723. [CrossRef] [PubMed]
31. Tsuei, C.C.; Kirtley, J.R. Pairing symmetry in cuprate superconductors. *Rev. Mod. Phys.* **2000**, *72*, 969–1016. [CrossRef]
32. Takagi, H.; Ido, T.; Ishibashi, S.; Uota, M.; Uchida, S.; Tokura, Y. Superconductor-to-nonsuperconductor transition in $(La_{1-x}Sr_x)_2CuO_4$ as investigated by transport and magnetic measurements. *Phys. Rev. B* **1989**, *40*, 2254. [CrossRef] [PubMed]
33. Kamimura, H.; Ushio, H. On the Interplay of Jahn-Teller Physics and Mott Physics leading to the occurrence of Fermi pockets without pseudogap hypothesis and *d*-wave high T_c superconductivity in underdoped cuprate superconductivity. *J. Supercond. Nov. Magn.* **2012**, *25*, 677. [CrossRef]